Research Article | Vol. 30, No. 11 / 23 May 2022 / Optics Express 17886
Optics EXPRESS

Characterization method and analysis of misalignments in micro-concentrator photovoltaic modules

LUIS SAN JOSÉ,* GUIDO VALLEROTTO, REBECA HERRERO, AND IGNACIO ANTÓN

Instituto de Energía Solar, Universidad Politécnica de Madrid, Avda. Complutense 30, 28040 Madrid, Spain
luis.sanjose@ies.upm.es

Abstract: Micro-scale concentrator photovoltaics (micro-CPV) is an emerging trend for the development of high-efficiency, low-cost photovoltaic systems. The miniaturization of optics and cells offers advantages in terms of performance and enables differentiation in the PV market. However, the sub-millimeter size of the solar cells used, the intrinsic narrow angular tolerance of CPV optical systems (typically around 0.5° and 2°), and the massive number of cells per module lead to very tight mechanical tolerances. Therefore, determining the misalignments between cells and optics is important for quality control inspection of modules. In this paper, we describe a method for characterizing these misalignments based on image acquisition and its subsequent processing and apply it to a micro-CPV module composed of 572 lens-cell units. This method is validated, using a unique experimental technique that takes advantage of the tracking system embedded in the module. The statistical distributions of misalignments are compared for two tracking positions, residuals are determined and shows the consistency of the method. Finally, the impact of misalignment distributions on the IV curve of the module is discussed.

© 2022 Optica Publishing Group under the terms of the Optica Open Access Publishing Agreement

1. Introduction

Concentrator Photovoltaics (CPV) maximizes the electrical generation per module area by concentrating sunlight into small high-efficient photovoltaic solar cells [1]. In this line, micro-concentrator photovoltaics (micro-CPV) downsizes module components to increase performance and potentially reduce the cost of electricity [2]. This also allows exploring unconventional approaches that would not be neither cost effective nor efficient in traditional macro-scale CPV due to large material consumption or high bulk absorption.

While concentrator modules must be aligned to the sun, the scale of micro-CPV allows the sun-tracking mechanism to be embedded in the module, instead of using a bulky external tracker structures. This is called integrated tracking [3], where relative displacements of a few millimeters between optics and cells keeps the light spot focused on the cell at different angles of incidence (AOI) [4–6]. Consequently, it is possible to mount micro-CPV modules featuring integrated tracking in fixed tilt position (*e.g.*, in rooftops as conventional PV), while preserving the superior efficiency of the CPV technology. The major advantage of the embedded tracker is that provides unique capabilities and market differentiation to conventional silicon flat modules [4]. Hybrid architectures, where the backplane is covered with monofacial or bifacial silicon cells, harvest separately Direct Normal Irradiation (DNI) and diffuse irradiance components providing superior efficiencies for area-constrained applications [7]; translucent architectures, where diffuse light is transmitted through the module and DNI can be either converted to electricity or transmitted through, provides added value for dual-land-use applications such as agrivoltaics, or for daylight control in building integrated photovoltaics.

#458337 https://doi.org/10.1364/OE.458337
Journal © 2022 Received 21 Mar 2022; revised 26 Apr 2022; accepted 28 Apr 2022; published 9 May 2022

Optics EXPRESS

The micro-scale implies a huge increase in the number of optics-cell units per square meter, and in turn a need for parallel assembly of the components in the module. Moreover, the mechanical tolerances in the manufacturing of micro-CPV modules are very tight, so high precision manufacturing processes are necessary to ensure accurate positioning of the optical components and the cells [8]. Misalignments among optics-cell units cause light leakages, reduce module fill-factor and degrade performance. Thus, inspecting and characterizing the misalignments between the module components may provide a valuable feedback and serve as a quality control tool on the production line [9,10].

Misalignments characterization of CPV modules has been widely described [11,12]. One such device, called Module Optical Analyzer [13,14] was conceived to be integrated in a solar simulator for quality control into a production line. However, this procedure does not have sufficient resolution for micro-CPV scale. Thus, an alternative procedure was proposed to be applicable to micro-CPV modules and described in [15,16]. The method consists of taking a photograph of each solar cell magnified through its corresponding optics. Then, the set of acquired images is processed to determine the relative position between each cell and its optics in pixels, which are converted to values of length or angle by applying a transfer function previously determined. The method has been successfully validated previously for conventional CPV by measurements and ray tracing simulations of a single lens-receiver unit [17].

In this work the authors take a step forward and apply the method to an entire micro-CPV Insolight module [18] that is composed by 572 optics-cell units, each one consisting of a biconvex hexagonal lens and a semi-dome optical secondary element attached to a square solar cell. The quantification of misplacements between cell and optics is particularly challenging because the image formation of the receiver through the anidolic biconvex lenses is very poor, particularly for misaligned units. We also share a new procedure developed for the validation of the method that takes advantage of the integrated-tracker system that displaces the receivers' backplane in X,Y,Z directions following a spherical trajectory with respect to the lenses plane. Two sets of measurements are carried out, one with optimum alignment and a second with the backplane strongly misplaced, determining the statistical distribution of residuals for the uncertainty quantification.

The paper is organized as follows: first, the application of the method to micro-CPV is explained, using the Insolight module as a particular case study. Second, the misalignments among the 572 units are determined for two positions of the internal tracking. Finally, as a result of the comparison of the two sets of measurements, the uncertainty of the method is obtained for the case example and the misalignments distributions impact on the IV curve of the module is discussed.

2. Methodology for misalignment characterization in micro-CPV modules

The first generation of Insolight module (Gen0), composed of 572 lens-receiver units (see Fig. 1), is used for the experimental validation of this study. The module integrates an internal tracking system composed by three actuators: two of them displace the backplane in XY direction (*i.e.*, coplanar to the lenses) with maximum travel of ±12mm, and the third one performs an angular XY rotation. The movement in Z direction is controlled by "guiding elements", which force the backplane to follow a spherical trajectory that is a function of the X and Y coordinates. The focal distance of the lens is 12.7mm, and therefore the relation between the AOI and the receiver displacement (performed by the integrated tracking) is about 5°/mm.

The array of lenses is composed by 64 pieces molded in PMMA and glued to a glass substrate. Each piece has 9 biconvex lenses shaped as regular hexagons of 8.34mm side, arranged in a 3×3 honeycomb structure. The receivers are formed by a 1mm side square multi-junction solar cell with a 1mm radius glass semi-dome attached to it. The array of lenses and the backplane of

Optics EXPRESS

Fig. 1. Gen0 Insolight modules installed onto the rooftop of the Institute of Solar Energy in Madrid.

receivers are manufactured separately, misalignments among units will rely only on mechanical tolerances.

The manufacturing process was not fully automated for Gen0, so the first batches of modules suffered from significant misalignments that were reduced in subsequent generations. The result is that the hundreds of optics-cell units composing the module do not have their optical axis perfectly aligned due to the mechanical tolerances in the manufacturing process. The misalignment in an optics-cell unit between its elements depends on the relative position between the center of a cell and its lens ($\Delta\rho$). A spatial misplacement between cell and optics is equivalent to a shift in the angular transmission function equal to the misalignment $\Delta\varphi$ (see Fig. 2); their relation is explained in [17].

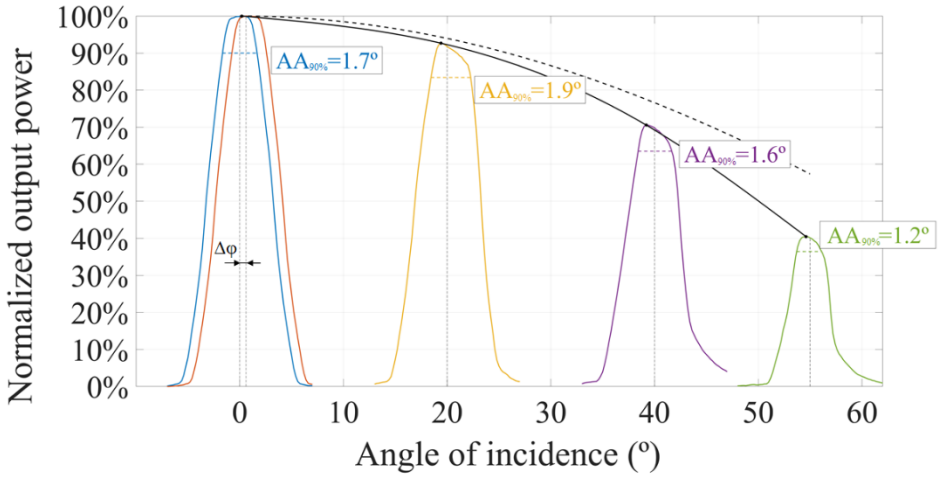

Fig. 2. Simulated angular transmission function of a single optics-cell unit of Insolight Gen0 for different incident angles (0°, 20°, 40° and 55°). Dotted line represents cosine response of the incident angle, and solid line the output power of the module at different angles of incidence. The acceptance angles AA for 90% power transmission degrades with the tracking position, particularly at large Sun incidence angles.

Optics EXPRESS

The angular acceptance ($AA_{90\%}$), defined as the angle at which the angular transmission decreases to X % of its maximum (where typically X = 90%), is a valuable figure of merit for CPV systems, because it describes the allowed tolerance for the tracking system and the stiffness requirement of the installation. In this regard, it is necessary to keep the AA as large as possible at the module level, ideally as the AA of a single optics-cell unit. Misalignments among units degrade the acceptance angle of the whole [19] and IV curve fill factor. In this regard power losses in the range of 10% are unacceptable, so misalignments should be kept well below $AA_{90\%}$, for instance to $AA_{98\%}$ (accounting only for 2% power losses) [20].

The Insolight optical system provides a wide acceptance angle ($AA_{90\%} = \pm 1.7°$) at normal incidence of the light, and keeps the light focused at a wide range of incident angles. The internal tracking locates the receivers at the optimum position, under the concentrated light spot, at each sun angle of incidence. Figure 2 shows the angular transmission function of a single optics-cell unit, simulated by ray tracing, considering:

- Normal light incidence, AOI = 0°, and the cell at the optimum position, in blue.
- Normal light incidence, AOI = 0°, and the cell misplaced Δρ producing a misalignment of Δφ in the optics-cell unit, in red.
- Several angles of incident light and cell at the optimum position, AOI = 20° in yellow, AOI = 40° in purple, and AOI = 55° in green.

The dotted black line accounts for the power loss related to the cosine of the incident angle of light, whereas the solid black line represents the actual power output of the module at which the angular transmittances are normalized. Figure 2 shows how the AA varies depending on the angle of incidence, slightly increasing from 1.7° to 1.9° at AOI = 0° and AOI= 20°, but decreasing to 1.2° at 55°, which means that misalignments could be more critical for high incident angles.

The measurement set up for the misalignments characterization is composed by a motorized XYZ stage where a camera with a macro lens is mounted, details can be found in [21]. The camera is moved in XY directions (*i.e.*, parallel to the lenses plane) to be placed in front of the center of each of the 572 optics-cell units; then a picture of the CPV lens and another of the cell magnified through the CPV lens are taken. Both cell and lens centers are determined through image processing, being the difference between centers equal to the spatial misalignment Δρ in pixels (see Fig. 3.c). This spatial misalignment (Δρ) can be translated into an angular value through a proportional pixels-to-degrees constant. This constant (°/px) may be calculated through simulations or measurements, assigning an angular size to the cell size [17].

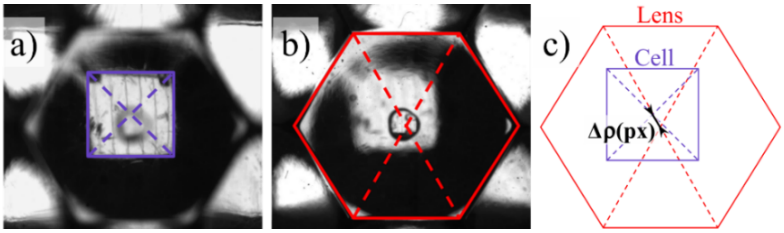

Fig. 3. a) Image in EL of the magnified cell (and the result of its processing through the square recognition and center detection); b) Image in EL of the lens (and the result of its processing through the hexagon recognition and center detection; c) Definition of the spatial misalignment Δρ as the difference between the lens and cell centers.

The following conditions are relevant for a correct image acquisition and successful determination of the misalignments. First, the macro lens used along with the camera magnifies

Optics EXPRESS

both lens and cell in the image but narrows the depth of field. Thus, it is not possible to focus simultaneously both and identify their positions in the same photograph with the needed accuracy. Therefore, two pictures per lens-cell unit are taken varying only the camera focus to observe sharply the cell and the lens edges (Fig. 3.a and b respectively). Second, the anidolic design of the CPV lens of Insolight blurs the cell edges and deforms cell shape differently depending on the misalignment of the unit. So, current is injected into the cells to produce electroluminescence (EL) and enhance image contrast and ease the edge detection of the different elements.

A proper image processing is essential to minimize the uncertainty in the determination of the position of lenses and cells [21]. For the example case, a cell misplacement of 200 µm is equivalent to 1° misalignment in the angular transmission function and corresponds to hardly 100 pixels in the captured high-definition images (4904×3280px), where the cell has a size of nearly 800px. The processing aims, first, to enhance the hexagonal shape of the lens aperture and the square shape of the cell in the photographs (see Fig. 3), second, to determine their positions, and finally, to calculate the distance between both objects. The identification of the cell position requires different approaches depending on the observed deformation, which is in turn proportional to the cell displacement with respect to the center of its lens. Figure 4 presents examples of acquired images and its corresponding processing to show how the cell image segmentation (pink areas discerned from the background) and squared-shape features detection (*i.e.,* corners and edges marked as dots and dashed lines) works. The center of the cells positioned within tolerance, *i.e.*, misalignments limited to 1°, is perfectly determined (4 corners, 4 sides), but for those particular units with very large misalignments (*i.e.*, higher than 2°), only 2 sides are identified (Fig. 4.b) which leads to a higher uncertainty in the cell position. In a few other cases, the automated process was able to identify only one edge (Fig. 4.c), so cell position could not be determined. The numerical value of the misalignment for these last cases is not relevant as the cell position is far beyond tolerance (1.7°), but, for the sake of completeness, the cell position has been manually detected in these cases.

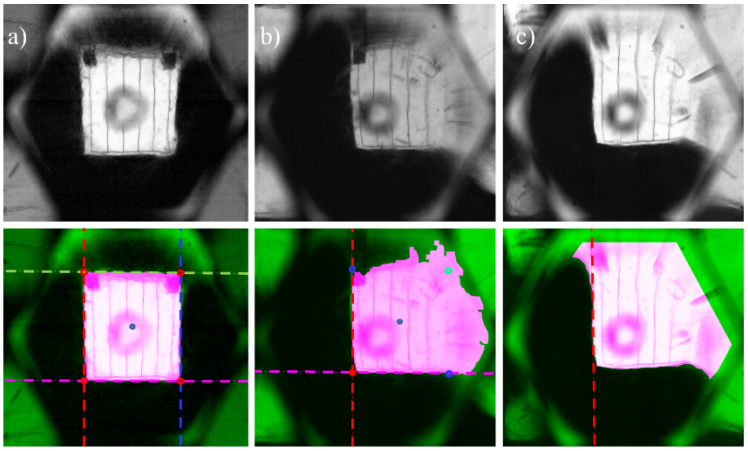

Fig. 4. Upper row: original images of cells magnified through the CPV lenses. Lower row: processed images. a) Cell image correctly processed, where the cell area (in pink) is properly segmented, the 4 corners and the 4 edges are well detected. b) Cell image processing in which the segmentation does not obtain straight edges and 2 corners are missing. The center is calculated considering the two detected corners and their projected distance. c) Fail in the cell image processing as the cell position is far beyond tolerance limits.

Optics EXPRESS

3. Validation of the method through repeatability study–uncertainty associated to camera position

For this measurement, the accuracy of the XYZ stage to position the camera centered with respect to the micro-CPV lens does not have a direct impact on the uncertainty of the method, since the cell position is determined with respect to the lens position (based on two different pictures taken with the same camera position). However, the image of the cell through the CPV lens is distorted depending on the camera position with respect to the center of the lens. Thus, it is desirable to take the picture with the camera as centered as possible with respect to the unit, avoiding important deformations of the cell shape. In order to account for this effect, an experiment has been performed in which the camera has been displaced in front of a single lens-receiver unit with steps of 0.25mm and a travel of ±0.75mm in X and Y axes. The standard deviation of the residuals (differences between the misalignment value for each camera position with respect to the one related to the camera centered) is 0.007° (see Fig. 5) which provides an idea of the corresponding uncertainty (*i.e.*, the method repeatability).

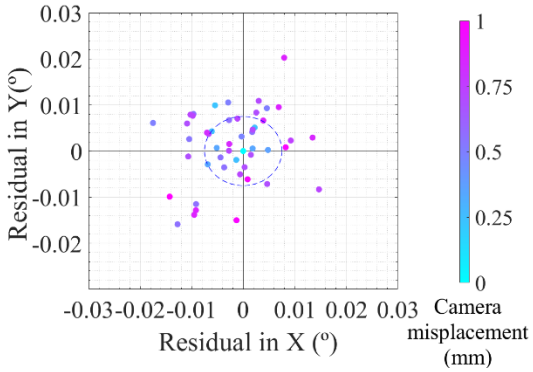

Fig. 5. Scatter plot of the residuals of the misalignments obtained placing the camera at 49 positions (scan range of ± 0.75mm with steps of 0.25mm). The standard deviation (circle) of the distribution is 0.007°.

4. Validation of the method through measurements of misalignments at 2 different integrated tracking positions

The main source of uncertainty of the method is determining the center of the cell by the processing above described, particularly when the image of the cell is strongly deformed. In order to account for this effect and to validate the proposed method, two set of measurements have been carried out as follows:

- In the first set of measurements the integrated tracking has been placed in the optimum position, *i.e.*, when the mean of statistical distribution of misalignments is zero. In this case most of the cells are fully segmented (4 corners and 4 edges are obtained).
- For the second set of measurements, a displacement of 200 μm has been introduced on the Y axis with respect to the first measurement by modifying the integrated tracking system position. This displacement corresponds to 1° offset in the angular transmission function in the Y direction. With this offset, some cells are largely misaligned, reaching values above 2°, which causes significant deformation in the images. The performance of the automated segmentation is poorer, 38 cells are segmented with only 2 corners and other 139 are manually segmented.

Optics EXPRESS

In both set of measurements, one photograph focusing the lens and other focusing the magnified cell are taken for each of the 572 module units. Each spatial misalignment value is determined according to the difference between lens and cell centers ($\Delta\rho$ in the measurement scheme in Fig. 3.c). The misalignment angular value ($\Delta\varphi$) is obtained multiplying the difference measured on the image by a pixels-to-degrees constant dependent on the set-up configuration, the camera characteristics and the module architecture, which is obtained empirically as explained in [17]. The displacement introduced in the Y direction does not modify the relative misalignment among units but introduces a 1° offset in the Y axis.

To show the impact of the misalignments distribution in the electrical performance, the Insolight module has been electrically characterized in the solar simulator under collimated light [22,23]. The IV curve for normal illumination and optimum placement of the integrated tracking has been measured. In this case, the optimum position for the integrated tracking is determined as the maximum power output obtained through an iterative scan in XY directions of the module backplane. Moreover, the IV curve of the module has also been measured by modifying the integrated tracking 200 µm in Y axis with respect to the optimum position.

5. Results and discussion

Figure 6 shows the X and Y spatial misalignments for both sets of experiments, only 1 quarter of the module is represented for the sake of comprehension (143 units), the other 3 exhibit similar results. The results are represented grouped by colors corresponding to pieces of 3×3 units of the lenses array (as shown in Fig. 6.a). The differences between lens and cell centers detected in the first set of measurements (optimum tracking position) are represented with filled circles, while for the case of the second set (200 µm displacement in Y direction) are represented as unfilled squares, both expressed in pixels. As it can be observed, the spatial misalignments (see Fig. 3.c) practically coincide for the X axis (Fig. 6.b up) for both sets, whereas a positive offset is observed in Y axis for the second measurement (Fig. 6.b low).

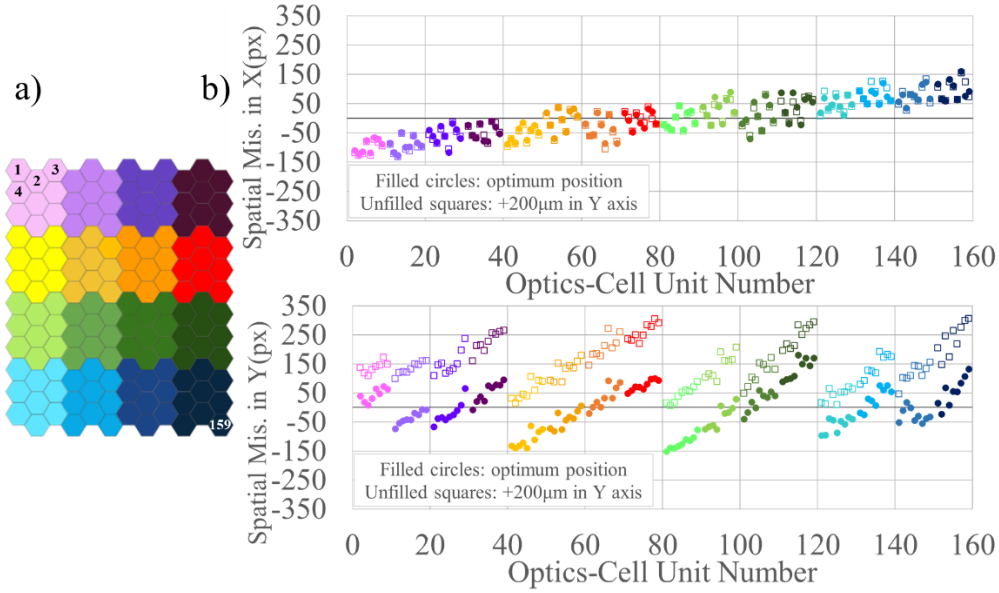

Fig. 6. a) Layout of the lens array pieces for one module quarter. b) X(upper) and Y(lower) spatial misalignment detected in both measurements for the first module quarter.

Optics EXPRESS

As stated, a spatial misalignment between a single cell and its optics is equivalent to an angular shift in the angular transmission function of that unit with respect to the others, degrading the overall performance of the module, more details can be found in [1,9,14 and 19].

Figure 7 shows the misalignment values of the whole module, in angular units, represented as a scatter plot, Fig. 7.b for the first set (optimum tracking position) and Fig. 7.c for the second (200 µm displacement in the Y axis from optimum tracking position, corresponding to 1°). In both graphs the circles indicate the $AA_{90\%}$ and $AA_{98\%}$ of a single optics-cell unit. The units are colored accordingly to the 4 quarters of the module, as detailed in Fig. 7.a. The applied image processing performs automatic corrected segmentation (as shown in Fig. 4) to detect the lens and cell positions for most but not all units. Those that are manually processed are represented as unfilled markers in Fig. 7.

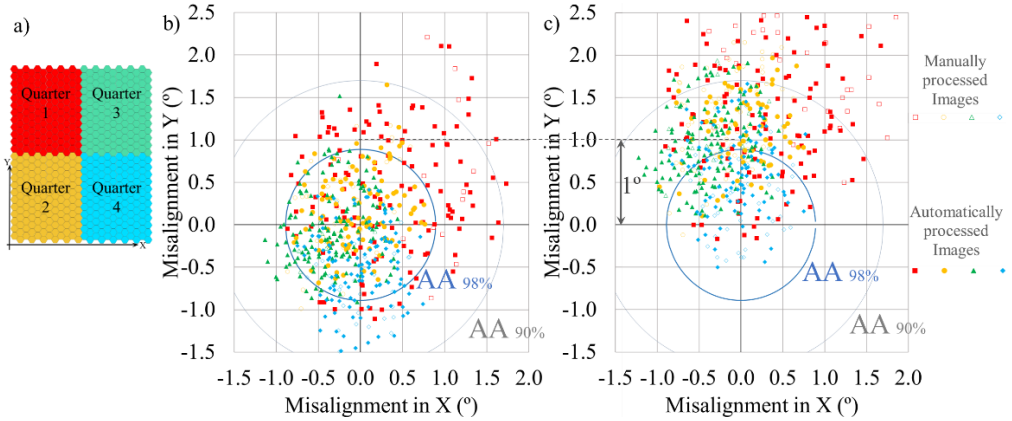

Fig. 7. a) Module is divided in 4 quarters (one color for each) with 572 lens-cell units in total b) Measured misalignments for a fixed optimum tracking position. c) Measured misalignments with introduced Y offset of a 200 µm (equivalent to 1°).

To evaluate the uncertainty of the method, the difference between misalignments for the 572 lens-cell units, in both set of measurements, is analyzed. Firstly, the 1° offset in Y of the second set is subtracted and then, the difference of each pair of values for each unit misalignment from the two set of measurements is calculated. The result is a set of 572 deviations in X and Y axes, which are fitted to Gaussian distributions (Fig. 8.a). Both X and Y distributions have a standard deviation of 0.1° (which corresponds to a cell displacement of 20 µm) when all units are considered, and 0.08° when only the units with automatic segmentation are included. These values represent the uncertainty associated to the method, and they should be considered the worst case values, as a large displacement, such as 200 µm, causes cell photographs to be worse segmented due to deformations in the magnified cell, which increases the error in the determination of the cell position.

An important consideration must be done regarding the alignment between the XY axes of the module integrated tracking system and the XY axes of the camera moving system. A perfect alignment between both Cartesian XY systems is not necessary for the correct misalignment characterization, but it has a relevant impact on the presented experiment. The two sets of measurements have a displacement of 200 µm in the Y direction (accordingly to the XY axes of the internal tracker) and should be detected as a displacement only in the Y direction by the processed images. But if there is a slight rotation among both Cartesian XY systems, the images would detect it in the differences among both set of measurements. For the experiment, the XY system of the camera movement has been aligned with the module frame, which could be different than the XY system of the internal tracker. This rotation in both Cartesian systems

Optics EXPRESS

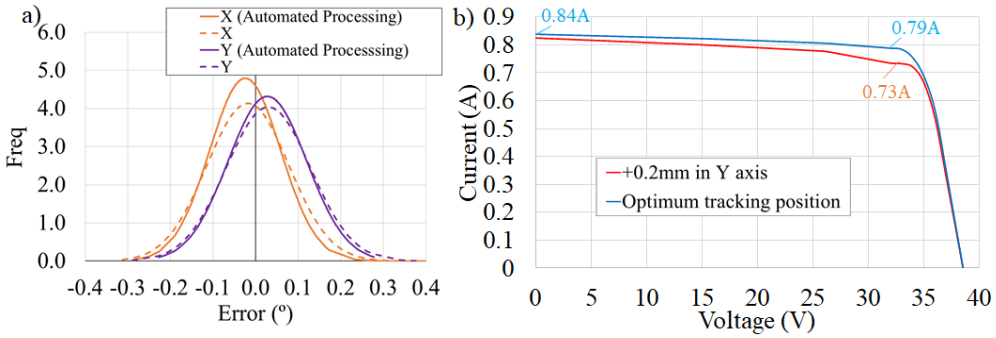

Fig. 8. a) Best fit Gaussian distribution of the differences between misalignments values determined with the two sets of measurements, taking into account all units (dotted line) and only the automatically processed units (solid line). b) IV curves measured for the integrated tracking position that maximizes the power output (optimum) and with the integrated tracking displaced 200μm (equivalent to 1°) in Y direction with respect to that optimum position.

emerges in the statistical distributions of the differences of measured values in both sets, which does not have zero mean, but is positive in Y (0.03°) and negative in X (-0.02°), as shown in Fig. 8.a.

The misalignment values with the internal tracking aligned (Fig. 7.b) are mostly within the acceptance angle $AA_{90\%}$, but a significant number of units exceed $AA_{98\%}$. The impact of the misalignments in the IV curve (Fig. 8.b, blue trace) is a significant slope (current ranges from 0.84A to 0.79A) and a power loss of 5.5%. It must be pointed out that the module has a first level of electrical connection of cells in parallel that reduces the impact of misalignments. If all cells were connected in series, power losses exceeding 10% would be expected accordingly to Fig. 7.b.

For the case of the backplane misplaced 200 μm (or 1°), there is a high number of cells with a misalignment above the $AA_{90\%}$ (Fig. 7.c), which leads to a higher slope in the IV curve (Fig. 8.b, red trace) so current drops to 0.73 A which corresponds to a power loss of 13%. It is noteworthy that, despite the acceptance angle $AA_{90\%}$ of the optical system is 1.7°, a displacement of the tracker as low as 1° causes a power degradation exceeding 10%, which means that there is a degradation of the $AA_{90\%}$ of the module compared to a single optical unit. It would be desirable to delimit the maximum misalignments to values below $AA_{98\%}$ to keep the high acceptance angle of the optics-cell unit at the module level. And what is more important for this technology, as the $AA_{90\%}$ decreases with the angle of incidence (see Fig. 2), the power losses associated to misaligned cells will increase for higher sun incident angles, which will in turn lead to a reduction in the energy yield of the module.

6. Conclusions

A method based on image processing for misalignments characterization of optics-cell units, which was conceived for conventional CPV, has been successfully applied to a micro-CPV module based on Insolight technology. The measurement set-up has been implemented based on a XYZ stage and a camera with a macro lens. Two images are captured, one focusing the CPV lens aperture and a second focusing the cells magnified by its CPV lens. The image processing for a correct automated detection of the lens and cell position has been developed.

The uncertainty of the method has been evaluated with an experiment where the misalignments of 572 optics-cell units where determined, taking advantage of the integrated tracking of the module. In a first set of measurements, the internal tracking was placed at the optimum position, in a second it was displaced 200 μm in the Y axis. The differences in the misalignment values

Optics EXPRESS

obtained for both sets were evaluated, providing a standard deviation of 0.08° (less than 20 µm in the cell position), being an acceptable value to validate the method for quality control in the manufacturing of micro-CPV modules.

Finally, the IV curves for the two cases, cells at optimum position and with offset, were measured and compared to the misalignments distributions, showing the impact of the misalignments on the fill factor of the IV curve and the degradation of the angular tolerance of the module compared to the acceptance angle of a single optics-cell unit.

Funding. European Social Fund (P2018/EMT-4308); European Regional Development Fund (P2018/EMT-4308); Comunidad de Madrid (P2018/EMT-4308); Horizon 2020 Framework Programme (857775, Grant agreement).

Acknowledgments. This work has received funding from the European Union's Horizon 2020 research and innovation programme under grant agreement No 857775. This work has been also partially supported by Comunidad de Madrid Program MADRID-PV2 P2018/EMT-4308, with co-funding from Fondo Europeo de Desarrollo Regional (FEDER) and Fondo Social Europeo (FSE) – Unión Europea.

Disclosures. The authors declare no conflicts of interest.

Data availability. Data underlying the results presented in this paper are not publicly available at this time but may be obtained from the authors upon reasonable request.

References

1. M. Wiesenfarth, I. Anton, and A. W. Bett, "Challenges in the design of concentrator photovoltaic (CPV) modules to achieve highest efficiencies," Appl. Phys. Rev. **5**(4), 041601 (2018).
2. C. Domínguez, N. Jost, S. Askins, M. Victoria, and I. Antón, "A review of the promises and challenges of micro-concentrator photovoltaics," *AIP Conference Proceedings.* Vol. 1881. No. 1. AIP Publishing, (2017).
3. H. Apostoleris, M. Stefancich, and M. Chiesa, "Tracking-integrated systems for concentrating photovoltaics," Nat. Energy **1**(4), 16018 (2016).
4. G. Nardin, C. Domínguez, A.F. Aguilar, L. Anglade, M. Duchemin, D. Schuppisser, and I. Antón, "Industrialization of hybrid Si/III–V and translucent planar micro-tracking modules," Prog. Photovoltaics **29**(7), 819–834 (2021).
5. N. Jost, G. Vallerotto, A. Tripoli, B.D. L'Eprevier, C. Domínguez, S. Askins, and I. Antón, "Molded glass arrays for micro-CPV applications with very good performance," *AIP Conference Proceedings,* **2298**(1), 050003 (2020).
6. A. Ito, D. Sato, and N. Yamada, "Optical design and demonstration of microtracking CPV module with bi-convex aspheric lens array," Opt. Express **26**(18), A879–A891 (2018).
7. K. A. W. Horowitz, G. Nielson, D. W. Cunningham, Z. Majumdar, A. Ramdas, and B. Sigrin, "Revisiting the Effects of Photovoltaic Module Efficiency on Installed System Cost and Market Adoption," *2020 47th IEEE Photovoltaic Specialists Conference (PVSC)*, 2020, pp. 2054–2056.
8. K. Araki, K.H. Lee, N. Hayashi, K. Ichihashi, S. Kanayama, T. Inohara, and M. Yamaguchi, "Alignment tolerance control of the micro cpv array using Monte Carlo methods," In *2019 IEEE 46th Photovoltaic Specialists Conference (PVSC)* (pp. 0202–0209). IEEE (2019).
9. K. Araki, H. Nagai, R. Herrero, I. Antón, G. Sala, and M. Yamaguchi, "Off-Axis Characteristics of CPV Modules Result From Lens-Cell Misalignment Measurement and Monte Carlo Simulation," IEEE J. Photovoltaics **6**(5), 1353–1359 (2016).
10. R. Herrero, I. Antón, M. Victoria, C. Domínguez, S. Askins, G. Sala, and K. Araki, "Experimental analysis and simulation of a production line for CPV modules: impact of defects, misalignments, and binning of receivers," Energy Sci. Eng. **5**(5), 257–269 (2017).
11. R. Herrero, C. Domínguez, S. Askins, I. Antón, and G. Sala, "Luminescence inverse method for CPV optical characterization," Opt. Express **21**(S6), A1028–A1034 (2013).
12. R. Herrero, C. Domínguez, S. Askins, I. Antón, and G. Sala, "Two-dimensional angular transmission characterization of CPV modules," Opt. Express **18**(S4), A499–A505 (2010).
13. R. Herrero, S. Askins, I. Antón, G. Sala, K. Araki, and H. Nagai, "Module optical analyzer: Identification of defects on the production line," *AIP Conference Proceedings*, 1616, pp. 119–123 (2014).
14. R. Herrero, S. Askins, I. Antón, and G. Sala, "Evaluation of misalignments within a concentrator photovoltaic module by the module optical analyzer: A case of study concerning temperature effects on the module performance," Jpn. J. Appl. Phys. **54**(8S1), 08KE08 (2015).
15. L. San José, R. Herrero, I. Antón, and G. Sala, "Computer vision algorithm for relative misalignments estimation in CPV modules," In *AIP Conference Proceedings* 2012(1), 100004. AIP Publishing LLC (2018).
16. L. San José, R. Herrero, and I. Antón, "Relative misalignments estimation in on-tracker CPV modules through image processing," In *AIP Conference Proceedings* 2149(1), 080008. AIP Publishing LLC (2019).
17. L. San José, G. Vallerotto, R. Herrero, and I. Antón, "Misalignments measurement of CPV optical components through image acquisition," Opt. Express **28**(10), 15652–15662 (2020).
18. S. Askins, N. Jost, A.F. Aguilar, L. Anglade, G. Nardin, M. Duchemin, and I. Antón, "Performance of Hybrid Micro-Concentrator Module with Integrated Planar Tracking and Diffuse Light Collection," *2019 IEEE 46th Photovoltaic Specialists Conference (PVSC)*. IEEE, (2019).

Optics EXPRESS

19. I. Antón and G. Sala, "Losses caused by dispersion of optical parameters and misalignments in PV concentrators," Prog. Photovoltaics **13**(4), 341–352 (2005).
20. C. Domínguez, R. Herrero, and I. Antón, "Characterization of CPV Modules and Receivers," in *Handbook of Concentrator Photovoltaic Technology* (John Wiley & Sons, 2001).
21. L. San José, G. Vallerotto, R. Herrero, and I. Antón, "Misalignments characterization for micro-CPV modules," *AIP Conference Proceedings* **2298**(1) (2020).
22. C. Domínguez, S. Askins, I. Antón, and G. Sala, "Indoor characterization of CPV modules using the Helios 3198 solar simulator," *Proceedings of the 24th European Photovoltaic Solar Energy Conference* (2009).
23. C. Domínguez, I. Antón, and G. Sala, "Solar simulator for concentrator photovoltaic systems," Opt. Express **16**(19), 14894–14901 (2008).

91.161.190.146 {ts '2022-10-10 06:39:39'}